# Photochemical Control of Molecular Motion Associated with Pyramidal Inversion

**Alexander J. Hough,[a] Ivan Prokes,[a] James H. R. Tucker,*[b] Michael Shipman,*[a] and Tiffany R. Walsh*[a,c]**

[a] *Department of Chemistry, University of Warwick, Gibbet Hill Road, Coventry, CV4 7AL, UK. Fax: +44 2476 524112; Tel: +44 2476 523186; E-mail: m.shipman@warwick.ac.uk*

[b] *School of Chemistry, University of Birmingham, Edgbaston, Birmingham, B15 2TT, UK. Fax: +44 121 414 4403; E-mail: j.tucker@bham.ac.uk*

[c] *Institute for Frontier Materials, Deakin University, Waurn Ponds, 3216 VIC, Australia. Tel: +61 352 273 116; E-mail: tiffany.walsh@deakin.edu.au*

## Electronic Supplementary Information

## Experimental Procedures:

**2-[4-(4-Nitro-phenylazo)-phenylamino]-ethanol (4).**[1, 2]

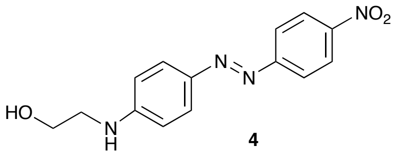

**4**

4-Nitroaniline (4.40 g, 31.9 mmol) was finely ground and dissolved in concentrated hydrochloric acid (32 mL) and water (240 mL) by vigorous stirring at room temperature for 3 h. The solution was then cooled to 0 °C and $NaNO_2$ (2.32 g, 33.6 mmol) added portionwise. The mixture was stirred at 0 °C for 1 h then used immediately in the azo coupling reaction. In a separate flask, β-hydroxyethyl aniline (5.00 g, 28.8 mmol) was dissolved in acetone (320 mL) and cooled to 0 °C. The diazo solution was added slowly over 20 minutes *via* dropping funnel maintained below 10 °C with ice. After addition, the red suspension was stirred for a further 1 h before acetic acid (1 mL) was added. The pH was adjusted to between 3 and 4 by dropwise addition of 10% sodium hydroxide. The precipitate was filtered, washed sequentially with hot and cold water then dried in a dessicator to give **4** (7.97 g, 97%) as a dark orange solid which was used without further purification. $^1$H NMR (400 MHz, $CDCl_3$) δ 3.44 (2H, q, $J$ = 4.9, C$H_2$), 3.93 (2H, q, $J$ = 4.9, C$H_2$), 4.73 (1H, s, N$H$), 6.72 (2H, d, $J$ = 9.0, Ar$H$), 7.89 (2H, d, $J$ = 9.0, Ar$H$), 7.93 (2H, d, $J$ = 9.0, Ar$H$), 8.33 (2H, d, $J$ = 9.0, Ar$H$); $^{13}$C NMR (100 MHz, $CDCl_3$) δ 45.4 ($CH_2$), 61.1 ($CH_2$), 112.5 (CH), 122.7 (CH), 124.7 (CH), 126.3 (CH), 145.0 (C), 147.6 (C), 152.1 (C), 156.6 (C); MS (ES$^+$) *m/z* 287 $[M+H]^+$. Data consistent with published values.[2]

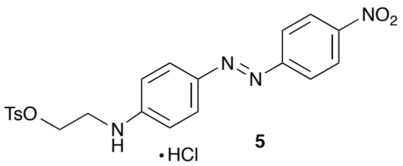

**5**

**[4-(4-Nitro-phenylazo)-phenyl]-[2-(toluene-4-sulfonyl-oxy)-ethyl]-amine hydrochloride (5).** To **4** (2.50 g, 9.20 mmol), tosyl chloride (27.8 g, 92.0 mmol) and DMAP (1.12 g, 9.20 mmol) in a round bottom flask was added pyridine (150 mL) precooled to –20 °C *via* cannula. The mixture was stirred at –20 °C (ethylene glycol / EtOH / $CO_{2\ (s)}$) for 6 h, then quenched with MeOH (100 mL). The solvent was removed *in vacuo* and the residual solid purified by column chromatography (10% acetone in petrol). The resulting free base was dissolved in a minimum volume of anhydrous benzene, then hydrogen chloride in diethyl ether was added dropwise to furnish **5** (331 mg, 8%) as a red solid. This material was contaminated with ca. 17% of the corresponding HCl salt of **4** as judged by $^1$H NMR, which could be removed after the next step. M.p. 110 °C (dec.); $R_f$ = 0.25; IR (thin film) 2813, 1614, 1557, 1508, 1392, 1336, 1259, 1167, 1142, 1101, 1010, 812, 661 cm$^{-1}$; $^1$H NMR (400 MHz, DMSO-$d_6$) δ 2.22 (3H, s, ArC$H_3$), 3.38 (2H, t, $J$ = 5.3, C$H_2$), 4.03 (2H, t, $J$ = 5.3, C$H_2$), 6.57 (2H, d, $J$ = 9.0, Ar$H$), 7.27 (2H, d, $J$ = 8.1, Ar$H$), 7.57 – 7.68 (4H, m, Ar$H$), 7.82 (2H, d, $J$ = 9.0, Ar$H$), 8.26 (2H, d, $J$ = 9.0, Ar$H$); $^{13}$C NMR (100 MHz, DMSO-$d_6$) δ 21.0 ($CH_3$), 41.0 ($CH_2$), 68.5 ($CH_2$), 122.8 (CH), 125.0 (CH), 125.5 (CH), 127.6 (CH), 128.3 (CH), 130.1 (CH), 131.8 (C), 143.2 (C), 144.7 (C), 146.8 (C), 153.0 (C), 156.0 (C); MS (ES$^+$) *m/z* 441 [M+H]$^+$; HRMS (ES$^+$) calcd. For $C_{21}H_{20}N_4O_5SNa$ = 463.1047 [M+Na]$^+$, found 463.1052.

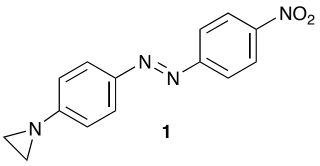

1

***trans*-(4-Aziridin-1-yl-phenyl)-(4-nitrophenyl)-diazene (1).**[3] To NaH (60% in mineral oil, 42 mg, 1.1 mmol), prewashed with dry petrol (3 x 1 mL) then dried under vacuum, was added a solution of **5** (100 mg, 0.21 mmol) in DMF (10 mL) at 0 °C *via* cannula. After stirring at 0 °C for 3 h, the mixture was quenched with $NH_4Cl$ (10 mL) and extracted with EtOAc (3 x 10 mL). The combined organics were washed with water (6 x 15 mL), dried ($MgSO_4$) and concentrated *in vacuo*. Purification by column chromatography (10% EtOAc in petroleum ether with 1% $Et_3N$) gave **1** (16 mg, 28%) as an orange solid. $R_f$ = 0.25 (10% EtOAc in petroleum ether with 1% $Et_3N$); IR (thin film) 2994, 1598, 1514, 1344, 1141, 1105, 851 $cm^{-1}$; UV $\lambda_{max}$: 262, 381, 391 nm; $^1H$ NMR (500 MHz, Toluene-$d_8$) δ 1.66 (4H, s, NC$H_2$), 6.78 (2H, d, $J$ = 8.7, Ar$H$), 7.59 (2H, d, $J$ = 9.0, Ar$H$), 7.85 (2H, d, $J$ = 9.0, Ar$H$), 7.88 (2H, d, $J$ = 8.7, Ar$H$); $^{13}C$ NMR (125 MHz, Toluene-$d_8$) δ 27.0 ($CH_2$), 121.1 (CH), 122.7 (CH), 124.2 (2 x CH), 148.1 (C), 148.3 (C), 155.6 (C), 159.6 (C); MS ($ES^+$) $m/z$ 291 $[M+Na]^+$; HRMS ($ES^+$) calc. for $C_{14}H_{12}N_4NaO_2$ = 291.0852, found 291.0857.

**Photochemical interconversion of 1→2: Optimisation Studies.**

| Solvent | Filter | T °C | Time (h) | Product ratio (*cis*-2:*trans*-1) |
|---|---|---|---|---|
| $CD_2Cl_2$ | <355 nm cut off (0.0012 M $BiCl_3$ in 2:3 conc. HCl:$H_2O$)[4] | rt | 1 | 0:100 |
| $C_6D_6$ | >360 nm cut off (0.8 M $NiSO_4$ + 1.0 M $CoSO_{4\,(aq)}$) | rt | 1 | 10:90 |
| $C_6D_6$ | <355 nm cut off (0.0012 M $BiCl_3$ in 2:3 conc. HCl:$H_2O$)[4] | rt | 1 | 17:83 |
| $C_6D_6$ | ~390 nm band pass (0.75% w/v $I_2$ in $CCl_4$)[5] | rt | 3 | 26:74 |
| $C_6D_6$ | ~390 nm band pass (0.75% w/v $I_2$ in $CCl_4$)[5] | <10 °C (ice / water) | 3 | 56:44 |
| Toluene-*d*$_8$ | ~390 nm band pass (0.75% w/v $I_2$ in $CCl_4$)[5] | <10 °C (ice / water) | 3 | 52:48 |
| Toluene-*d*$_8$ | ~ 390 nm band pass ( glass filter 50 mm$^2$ Schott FSQ-UG1) | <10 °C (ice / water) | 4 | 44:56 |

***cis*-(4-Aziridin-1-yl-phenyl)-(4-nitro-phenyl)-diazene (2)**.

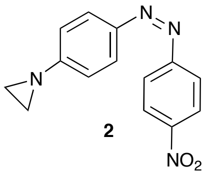

**2**

***Representative procedure:*** *Trans*-**1** (6 mg, 0.012 mmol) was dissolved in toluene-*d*$_8$ (0.6 mL) then filtered into an NMR tube. The tube was suspended at the front of a 2 L beaker containing ice / water. The tube was irradiated with a 125 W medium pressure mercury lamp through a window of glass bandpass filter focused around 390 nm (Schott FSQ-UG1 UV bandpass filter). After being irradiated for 4 h the sample was removed, and stored in ice, and immediately analysed by $^1$H NMR spectroscopy, which revealed it to be a 56:44 mixture of *trans* and *cis* isomers. Selected data for *cis*-**2:** $^1$H NMR (400 MHz, Toluene-*d*$_8$) δ 1.56 (4H, s, NC*H*$_2$), 6.32 (2H, d, *J* = 8.8, Ar*H*), 6.47 (2H, d, *J* = 8.8, Ar*H*), 6.64 (2H, d, *J* = 8.8, Ar*H*), 7.59 (2H, d, *J* = 8.8, Ar*H*).

**Thermal conversion of *cis*-2 → *trans*-1.** An NMR tube containing a 63:37 mixture of **1** and **2** (6 mg, 0.012 mmol) in toluene-$d_8$ (0.6 mL) was immersed in an oil bath at 60 °C for 10 minutes. Complete conversion to **1** was achieved as judged by $^1$H NMR spectroscopy.

The process of photochemical conversion and thermal reconversion was repeated three times in succession with no losses in conversion or degradation.

## UV-vis Spectra for 1

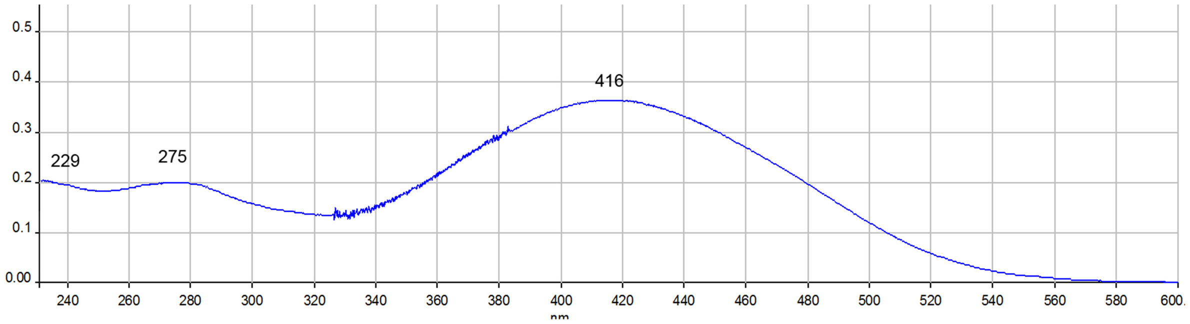

## Photochemical Apparatus

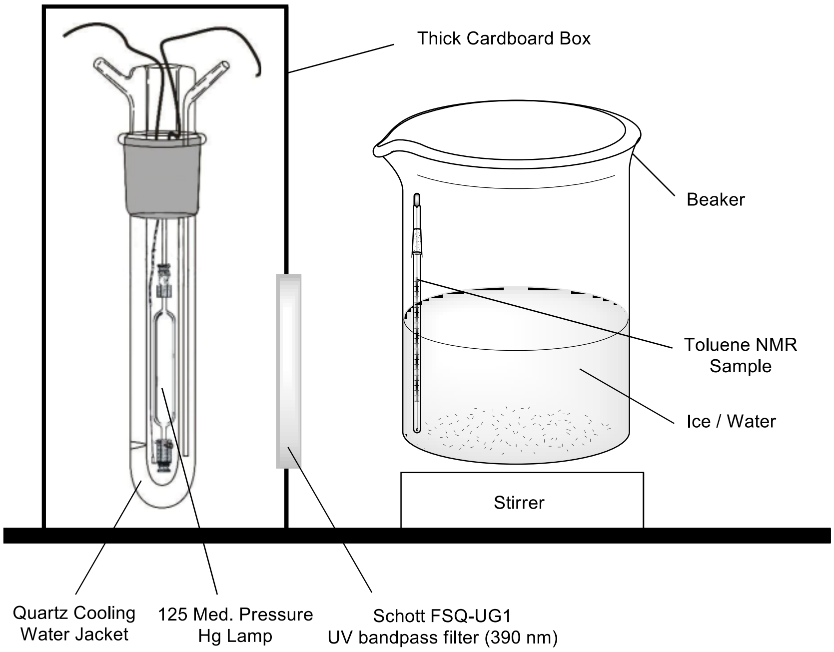

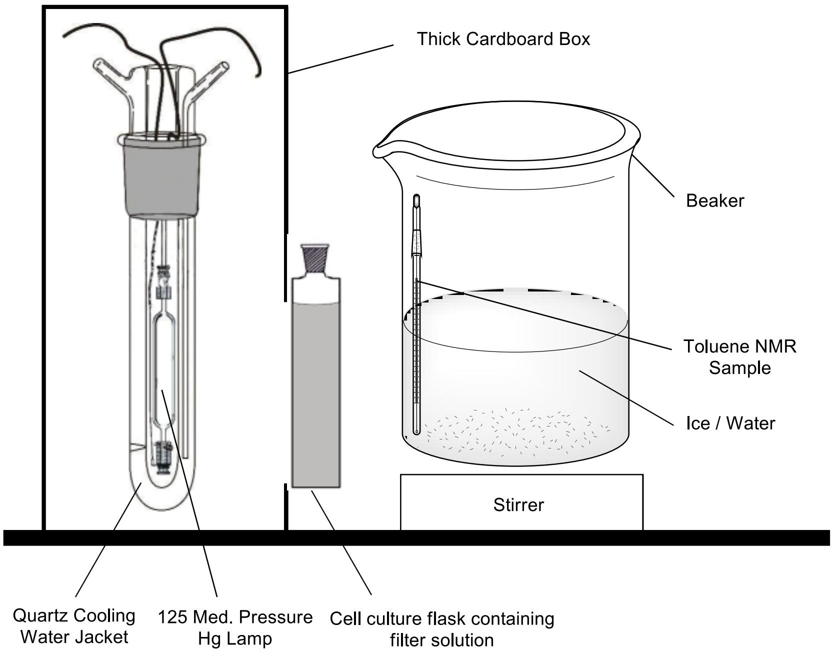

**Determination of activation parameters**. Variable temperature NMR spectra were recorded at 500 MHz on a Bruker DRX spectrometer in $d_8$-toluene. Natural line widths for each spectrum were determined by line fitting deconvolution with Mestrec-Nova. The chemical shifts of the corresponding exchangeable signals at close to coalescence were determined from a plot of $\upsilon_A$-$\upsilon_B$ (in Hz) vs T at temperatures well below coalescence. Simulated spectra for the $A_2X_2$ spin system were generated using the WINDNMR package (version 7.1.12)[6] and compared with the acquired spectra using difference spectra. From these simulations, the rate constant k for inversion were determined as a function of temperature. Hence, from the Eyring equation, the activation parameters could be determined by plotting ln(k/T) versus 1/T wherein:

$$\Delta H^{\ddagger} = -(\text{slope})R \text{ and } \Delta S^{\ddagger} = [\text{intercept} + \ln(h/K_b)]R$$

where R = gas constant; h = Planck's constant; and $k_b$ = Boltzmann's constant.

VT NMR spectra for *trans*-**1** [measured (left) and simulated (right)]:

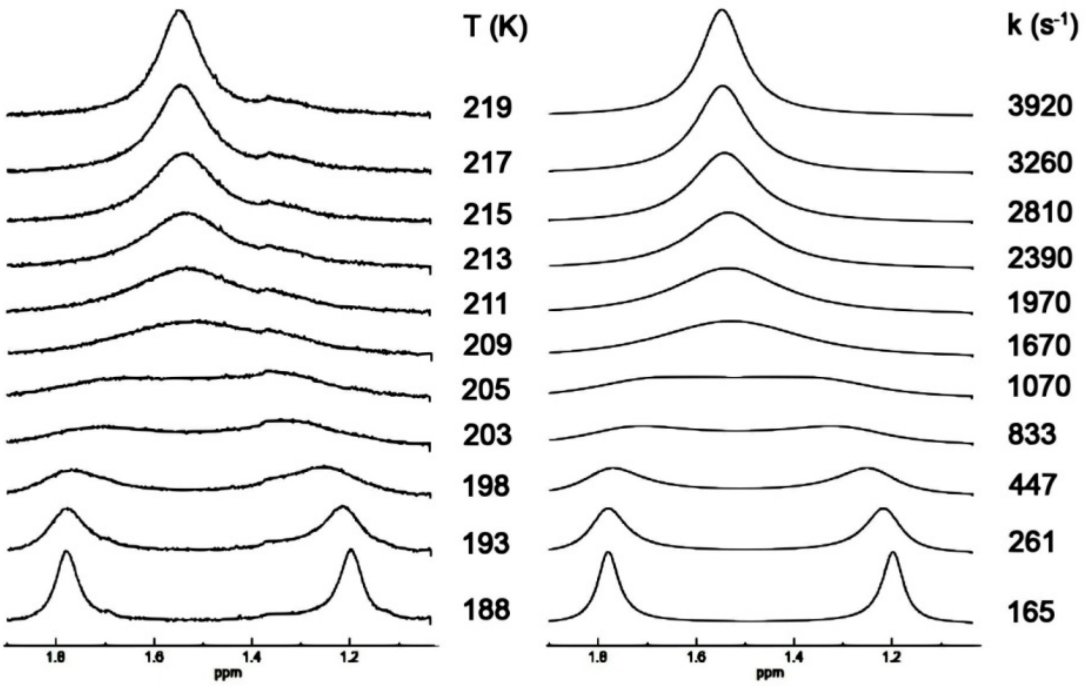

Corresponding VT NMR spectra for *cis*-**2** presented in Fig 2 of the paper.

## Eyring Plots and Activation Parameters

For **1:**

$\Delta H^{\ddagger}$ = 34.4±0.3 kJ mol$^{-1}$; $\Delta S^{\ddagger}$ = -16.3±1.6 J K$^{-1}$ mol$^{-1}$ and $\Delta G^{\ddagger}$ (at 298 K) = 39.2±0.8 kJ mol$^{-1}$.

| T (K) | k |
|---|---|
| 183 | 92.00 |
| 188 | 165.00 |
| 193 | 261.00 |
| 198 | 447.30 |
| 203 | 833.40 |
| 205 | 1069.50 |
| 207 | 1387.50 |
| 209 | 1674.30 |
| 211 | 1974.30 |
| 213 | 2394.40 |
| 215 | 2811.50 |
| 217 | 3263.50 |
| 219 | 3921.60 |
| 221 | 4771.60 |
| 223 | 5641.70 |
| 228 | 9141.70 |
| 233 | 13761.60 |
| 243 | 31611.70 |

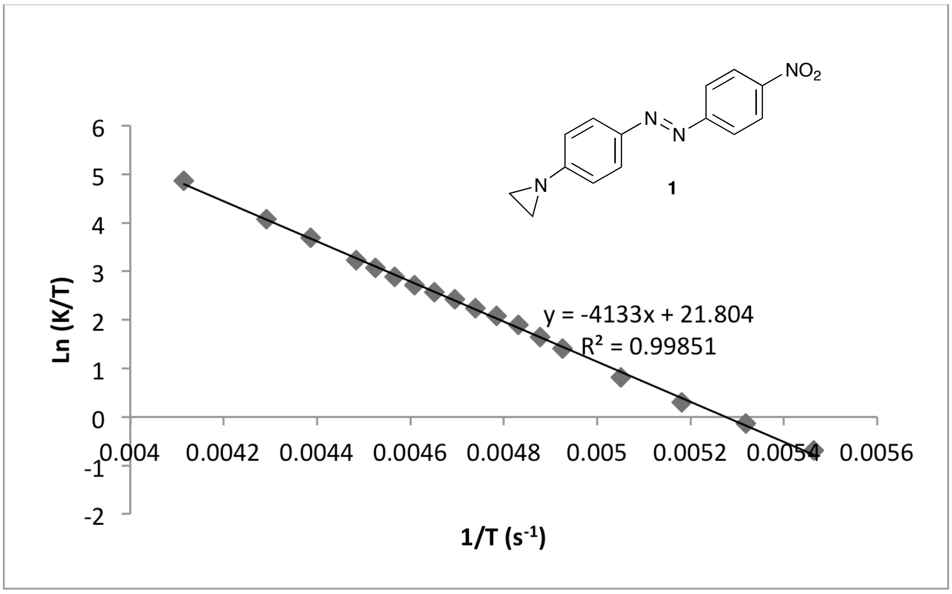

For **2:**

$\Delta H^{\ddagger}$ = 35.3±0.5 kJ mol$^{-1}$; $\Delta S^{\ddagger}$ = -21.4±2.1 J K$^{-1}$ mol$^{-1}$ and $\Delta G^{\ddagger}$ (at 298 K) = 41.7±1.1 kJ mol$^{-1}$.

| T (K) | k |
|---|---|
| 183 | 46.30 |
| 188 | 49.40 |
| 193 | 82.50 |
| 198 | 134.60 |
| 203 | 266.70 |
| 205 | 323.80 |
| 229 | 3133.80 |
| 231 | 3603.80 |
| 233 | 4493.80 |
| 238 | 7553.80 |
| 243 | 11583.80 |
| 253 | 23342.80 |
| 263 | 40502.80 |
| 273 | 61232.80 |

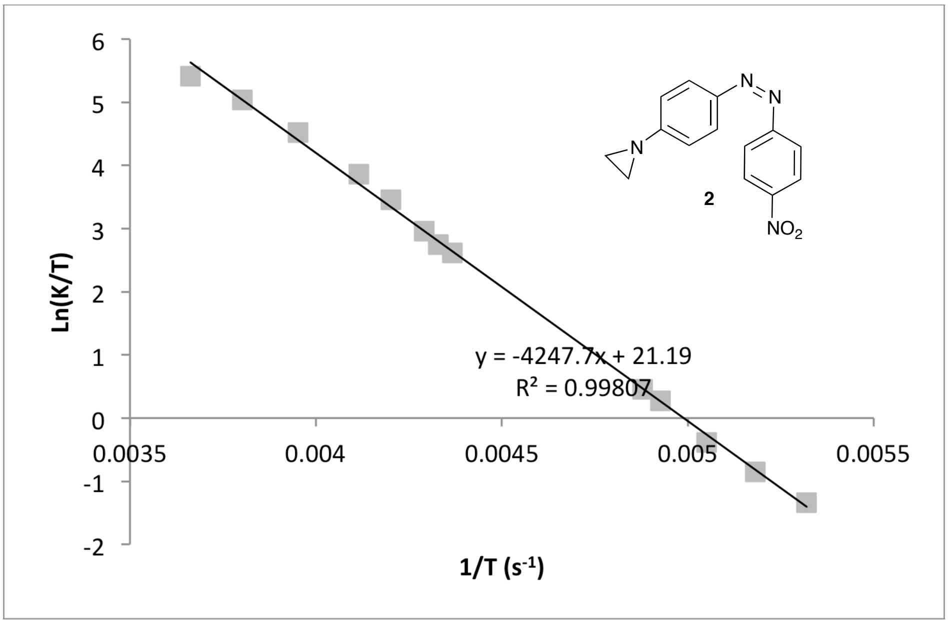

## Estimation of Errors in Line Shape Analysis

The most significant source of random error was assumed to originate in the line shape fitting to determine the activation parameters. As a plot of ln (k/T) vs 1/T is expected to yield a straight line, the linear regression model was applied to the data and the uncertainty in fit extracted using the ordinary least squares method in Microsoft Excel. This returned a >95% statistical significance for the experimental data along with the standard error in gradient and intercept. From this, the uncertainty in $\Delta G^{\ddagger}$, $\Delta H^{\ddagger}$ and $\Delta S^{\ddagger}$ can be estimated.

## $T_c$ Calculation Method

$\Delta G^{\ddagger}$ at coalescence derived using $\Delta G^{\ddagger} = RTc[23 + \ln(\frac{Tc}{\Delta\nu})]$

For **1**: $T_c = 207$ K and $\Delta\upsilon = 296.7$ Hz at 183 K

$$\Delta G^{\ddagger} \text{ @ } 207\text{ K} = 38.9\text{ kJ mol}^{-1}$$

For **2**: $T_c = 223$ K and $\Delta\upsilon = 288.9$ Hz at 183 K

$$\Delta G^{\ddagger} \text{ @ } 223\text{ K} = 42.2\text{ kJ mol}^{-1}$$

## Thermal isomerisation of 2 →1 monitored by $^1$H NMR spectroscopy

| Time (s) | Conv (%) |
|---|---|
| 300 | 52 |
| 2700 | 31 |
| 3360 | 24 |
| 3960 | 21 |
| 4560 | 19 |
| 5160 | 16 |
| 5760 | 15 |
| 6360 | 13 |
| 6980 | 12 |
| 7500 | 10 |
| 8160 | 7 |

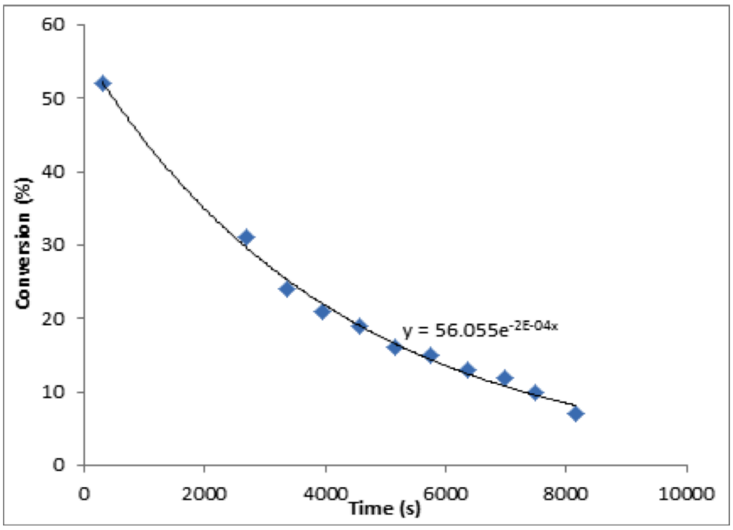

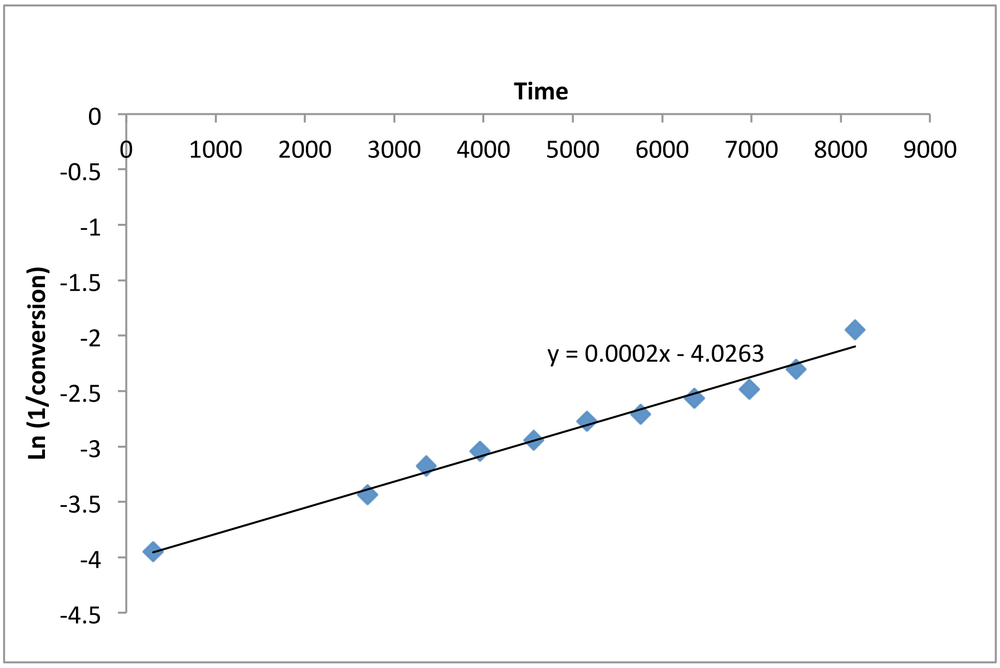

Hence, rate constant, $k = 2 \times 10^{-4}\ s^{-1}$

## Computational Modelling of 1 and 2:

All first-principles calculations were performed using the GAUSSIAN09[7] package, with all geometry optimization calculations employing analytic first and second-derivatives of the potential energy at every optimization step.

All four structures (one minimum and one transition-state each for **1** and **2**) were first optimized in the gas-phase at the MP2/6-31G* level of theory.

At this level of theory we performed systematic searches over possible ground state (GS) structures by considering the full range of possible rotamers supported by these compounds, given the *cis* and *trans* conformations. This amounts to exploring the possible dihedral angles around the C-N bond that connects each ring to the central azo group. We denote dihedral $\boldsymbol{\tau}\mathbf{1}$ corresponding with the ring associated with the nitro group, and dihedral $\boldsymbol{\tau}\mathbf{2}$ corresponding with the ring associated with the aziridine.

In the *trans* case (**1**), the conformer with both rings parallel to the plane of the azo group was found to be the GS. In the *cis* case (**2**), we found two almost iso-energetic structures for the GS: in isomer 1, $\boldsymbol{\tau}\mathbf{1} = 134^{\circ}$ and $\boldsymbol{\tau}\mathbf{2} = -49^{\circ}$; in isomer 2, these values were $\boldsymbol{\tau}\mathbf{1} = -134^{\circ}$ and $\boldsymbol{\tau}\mathbf{2} = 49^{\circ}$. The energy difference between these two isomers was 0.3 kJ/mol at the MP2/6-31G* level of theory, with isomer 2 being the lowest in energy of the two. This means that pyramidal inversion of the aziridine nitrogen in **2** facilitates interconversion in the *cis* structure between isomer 2 to isomer 1 and vice-versa (see Fig 1).

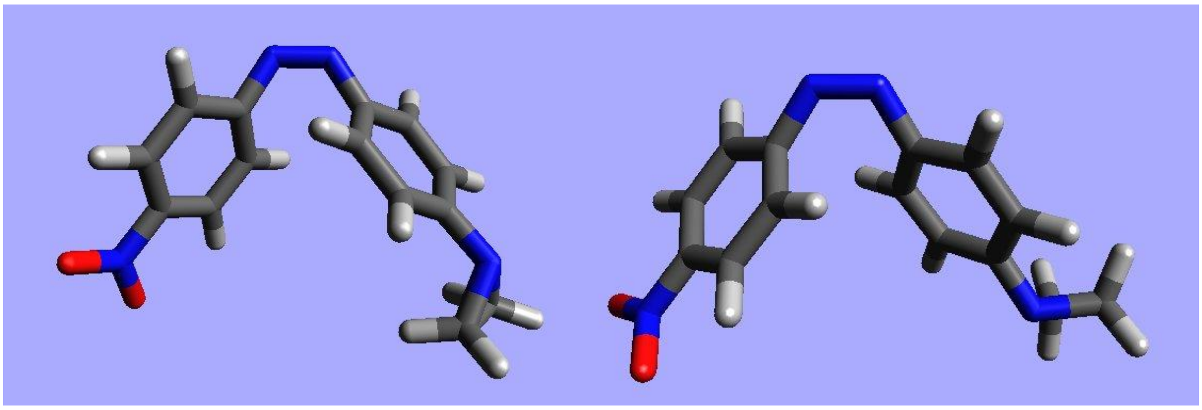

***Fig 1:*** *The two isoenergetic isomers of* ***2****. Left, isomer 1. Right, isomer 2.*

We identified the transition-state (TS) structures associated with pyramidal nitrogen inversion in **1** and **2** using the geometry optimization procedure outlined above. In each case, the transition vectors were inspected to confirm the mechanism of interconversion.

We then took these gas-phase structures obtained at the MP2/6-31G* level, and reoptimized each one in implicit solvent, using the polarizable continuum model (PCM) of Tomasi and co-workers.[8] The implicit solvent model in GAUSSIAN09 was configured to model toluene, so as to represent a general non-polar solvent. Again, for the TS structures we confirmed that in each case these were true first-order saddles on the potential energy landscape, corresponding with pyramidal nitrogen inversion in the aziridine.

Further, we took these implicit-solvent optimized structures and used these in single-point energy (SPE) calculations at the MP2/aug-cc-pVDZ level of theory (*i.e.* we performed MP2/aug-cc-pVDZ//MP2/6-31G* calculations). To estimate the change in Gibb's free energy in our barriers for **1** and **2**, we used the contributions from the vibrational frequencies, calculated at the MP2/6-31G* level (via the analytic vibrational frequencies) and added these to our potential energies obtained at the MP2/aug-cc-pVDZ//MP2/6-31G* SPE level.

**Natural Bonding Orbital (NBO) Analysis:** To gain a deeper insight into the electronic properties of **1** and **2**, we carried out a natural bond orbital (NBO) population analysis[9] at the MP2/aug-cc-pVDZ level, for both the GS and TS structures of **1** and **2**.

The delocalization of electron density from the nitrogen lone-pair to the adjacent ring stabilizes the donor-acceptor interaction. The corresponding second-order perturbation theory analyses of the Kohn-Sham equations indicate a stabilisation energy of 22.8 kJ/mol vs. 21.8 kJ/mol, for the GS of **1** and **2** respectively. Similarly, these stabilisation energies for the TS of **1** and **2** were 69.1 kJ/mol vs. 66.3 kJ/mol respectively. Taken together, these data suggest the following. First, these data indicate reduced levels of donation from the nitrogen lone-pair into the adjacent ring for **2** compared with **1**, in both the GS and TS (*i.e.* $21.8 < 22.8$, and $66.3 < 69.1$). Second, our NBO calculations show a greater change in delocalisation stabilisation energy in moving from the GS → TS for **1** ($69.1 - 22.8 = 46.3$ kJ/mol) compared with **2** ($66.3 - 21.8 = 44.5$ kJ/mol).

## References

[1] G. Hallas and J. H. Choi, *Dyes Pigm.* 1999, **40**, 99.

[2] M. R. Yazdanbakhsh, M. Giahi, and A. Mohammad, *J. Mol. Liq.,* 2009, **144**, 145.

[3] G. Hallas and M. A. Jalil, *Dyes Pigm.* 1992, **20**, 13.

[4] H. E. Zimmerman, *Mol. Photochem.,* 1971, **3**, 281

[5] S. L. Murov, in *Handbook of Photochemistry,* M. Dekker, New York, 1973

[6] H. J. Reich, "WinDNMR: Dynamic NMR Spectra for Windows." *J. Chem. Educ.* Software, 1996, **3D**, 2.

[7] Gaussian 09, Revision A.1, M. J. Frisch, G. W. Trucks, H. B. Schlegel, G. E. Scuseria, M. A. Robb, J. R. Cheeseman, G. Scalmani, V. Barone, B. Mennucci, G. A. Petersson, H. Nakatsuji, M. Caricato, X. Li, H. P. Hratchian, A. F. Izmaylov, J. Bloino, G. Zheng, J. L. Sonnenberg, M. Hada, M. Ehara, K. Toyota, R. Fukuda, J. Hasegawa, M. Ishida, T. Nakajima, Y. Honda, O. Kitao, H. Nakai, T. Vreven, J. A. Montgomery, Jr., J. E. Peralta, F. Ogliaro, M. Bearpark, J. J. Heyd, E. Brothers, K. N. Kudin, V. N. Staroverov, R. Kobayashi, J. Normand, K. Raghavachari, A. Rendell, J. C. Burant, S. S. Iyengar, J. Tomasi, M. Cossi, N. Rega, J. M. Millam, M. Klene, J. E. Knox, J. B. Cross, V. Bakken, C. Adamo, J. Jaramillo, R. Gomperts, R. E. Stratmann, O. Yazyev, A. J. Austin, R. Cammi, C. Pomelli, J. W. Ochterski, R. L. Martin, K. Morokuma, V. G. Zakrzewski, G. A. Voth, P. Salvador, J. J. Dannenberg, S. Dapprich, A. D. Daniels, Ö. Farkas, J. B. Foresman, J. V. Ortiz, J. Cioslowski and D. J. Fox, Gaussian, Inc., Wallingford CT, 2009**.**

[8] M. T. Cancès, B. Mennucci and J. Tomasi, *J. Chem. Phys.* 1997, **107**, 3032; M. Cossi, V. Barone, B. Mennucci and J. Tomasi, *Chem. Phys. Lett.* 1998, **286**, 253; B. Mennucci and J. Tomasi, *J. Chem. Phys.* **1997**, *106*, 5151.

[9] J. P. Foster and F. Weinhold, *J. Am. Chem. Soc.*, 1980, **102**, 7211.